Radiation Effects on a Radiation Tolerant CMOS Active Pixel Sensor

Gordon R. Hopkinson, Member, IEEE, Ali Mohammadzadeh and Reno Harboe-Sorensen

***Abstract*-- A comprehensive cobalt60, proton and heavy ion evaluation of the Fillfactory STAR-250 CMOS active pixel sensor has been performed for space applications up to 100 krd(Si). It was possible to eliminate image lag by adjustment of the bias voltage and this allowed a reduction in proton-induced dark signal. Both cobalt60 and proton irradiation produced a decrease in responsivity, which is thought to be due to total dose effects. There was also an increase in photoresponse nonuniformity (PRNU). No major single event effects (latch-up or functional interrupt) where seen at the maximum LET of 68 MeV/(mg/ cm^2).**

I. INTRODUCTION

ACTIVE pixel sensors (APSs) are starting to replace CCD imagers in many applications. Although the readout noise tends to be higher and the dark signal fixed pattern not as uniform, they have the advantage of dissipating less power and requiring lower clock voltages. Use of CMOS technology often means that additional functions (such as analogue to digital conversion) can be accommodated on-chip. Because the signal is readout from each pixel directly, the APS, unlike the CCD, does not suffer from charge transfer degradation and so has the potential for improved radiation tolerance. On the other hand, there is also the potential for mechanisms not seen in CCDs, such as parasitic (field oxide) leakage, single event latch-up (SEL) and single event functional interrupt (SEFI). Since the pixel structure is quite different, there is also the possibility for performance parameters to behave differently for APSs, compared with CCDs.

This paper reports the results of an evaluation of the STAR-250 sensor from Fillfactory NV, Belgium. This is a second generation device, the previous version having been evaluated in an earlier programme [1], where it was found that the sensor suffered from increases in leakage current at ~ 6 krd(Si) and changes in responsivity (both of which annealed). In addition, the on-chip 8-bit ADC was seen to latch up at an LET of 19.9 MeV/(mg/cm^2). The new version (STAR-250) has been hardened by design, through use of enclosed, gate-all-around NMOS transistors, plus a thin epitaxial layer and frequent well and substrate contacts to give latch up immunity. Crosstalk (and MTF) is improved through the use of four photodiodes per pixel and the ADC was replaced by a 10-bit version. Total ionizing dose tolerance has been verified for pixel test structures [2] and for a sensor used in a video camera [3]. Recently the manufacturer has presented both cobalt60 and proton data on complete STAR-250 devices [4]. Reference [2] discusses the trade-offs involved in the hardened design.

In the present evaluation the STAR-250 was subjected to cobalt60, proton and heavy ion irradiation in order to confirm the improved radiation tolerance of the device. The sensor is already being designed into instruments for space applications [5]. Another device from Fillfactory (the IRIS-2) was evaluated for SEL only, during the heavy ion testing. This device is interesting since it contains clock sequencing circuitry on-chip ('camera-on-a-chip').

In the course of the work it was discovered that the image lag and dark current performance of the STAR-250 can be greatly improved by a change to the operating bias and a study of the tradeoffs involved formed a major part of the study. Also important was the definition of a test methodology for assessing the performance in a heavy ion environment. Other examples of APS radiation testing can be found in [6]-[12].

II. EXPERIMENTAL

The STAR-250 [13] has 512 by 512 pixels on a 25 μm pitch, manufactured using Alcatel Microelectronics 0.5 μm CMOS technology. The chip has facilities for windowing and electronic shuttering. There is fixed pattern noise reduction circuitry and an on-chip 10-bit ADC, operable up to 5 MHz. Readout noise is typically 60-70 electrons rms (dominated by kTC noise). The device hardening resulted in a reduction in the fill factor but a value of 63% was still achieved by the manufacturer and this compares well with other APS designs.

Cobalt60 and heavy ion irradiations were carried out using a specially constructed bias board. This could power (and clock) the devices and monitor the power supply voltages and the video output (sending data to be logged by a PC). For heavy ion testing, a data processing module (based on a Xilinx SPARTAN FPGA) could be plugged into the board to

Manuscript received 10 September, 2003. This work was funded by the European Space Agency.

Gordon Hopkinson is with Sira Electro-Optics Ltd, South Hill, Chislehurst, Kent, BR7 5EH, UK (telephone +44 (0)208 468 1794, e-mail: gordon.hopkinson@siraeo.co.uk).

Ali Mohammadzadeh is with the European Space Agency, ESTEC, Keplerlaan 1, 2200 AG, Noordwijk, The Netherlands (telephone + 31 71 565 5894), e-mail ali.mohammadzadeh@esa.int.

Reno Harboe-Sorensen is with the European Space Agency, ESTEC, Keplerlaan 1, 2200 AG, Noordwijk, The Netherlands (telephone + 31 71 565 3883), e-mail Reno.Harboe.Sorensen@esa.int

perform histogramming of ADC data and detection of noise transients and single event interrupts. For this test the ADC was connected not to the video output of the sensor but to a commandable voltage from a digital to analogue convertor (DAC). If the device currents exceeded a given (programmed level) then the power was automatically cycled and the event logged to a file (in order to detect SEL events). Because the data processing module was expected to be radiation soft, it was removed during the cobalt60 and proton irradiations.

The cobalt60 irradiations were carried out at ESA, ESTEC at a dose rate of ~ 3 krd(Si)/hour. Monitoring of images and power supply currents during the test showed no significant changes and all devices were irradiated up to the maximum planned dose, which was 79.2 krd(Si). Three devices were irradiated biased and one unbiased.

Two further devices were irradiated with 9.5 MeV protons at the Tandem Van de Graaff accelerator at Ebis Iotron Ltd, Harwell, UK, both unbiased (pins shorted). The devices were masked with 1.5 mm Al plates to achieve dose regions of 0, 1, 10 and 100 krd(Si). The ADC and column amplifiers were masked so as not to be irradiated. Two more devices were irradiated at the heavy ion facility (HIF) at Louvain-la-Neuve, Belgium. During this test two IRIS-2 devices were also evaluated for SEL.

All the irradiations were carried out during the period May-November 2002. Dosimetry was carried out by the facility staff involved and is believed to be accurate to ±5%.

Electro-optical performance tests were carried out at Sira using a custom built evaluation system with programmable bias and clock levels (and timing sequences) and a 14/16 bit video digitization board. Tests were made both with the internal (10-bit) ADC and with the external digitization card.

III. Results

Measurements were made of linearity, threshold voltages, power supply currents, ADC integral and differential nonlinearity, dark signal, responsivity and response nonuniformity. The value of the charge to voltage conversion factor was taken as the manufacturer's datasheet value of ~ 5µV/electron, which was in line with Cd109 X-ray calibrations (when the lag effect was suppressed).

A. Effect of V_{pixel} Voltage

During the course of the testing it was discovered that, like many photodiode sensors, the STAR-250 suffers from image lag if operated under normal bias. This is particularly noticeable at low signal levels. Fig. 1 is a block diagram of a pixel, showing the four photodiodes and three-transistor (3T) architecture for reset and readout. A feature of the 3T arrangement is that the reset transistor operates in the 'sub-threshold' region at the end of the reset period [14],[15]. This can happen because the reset transistor and the analogue supply rail both have the same voltage (e.g. 5 V). The reset transistor will have a finite threshold voltage (typically about 1 V) and when the voltage across it falls below that level the transistor will start to cut off (and operate in the 'sub-threshold' region). In this case the reset is 'soft' and the photodiode and the reset drain do not reach thermal equilibrium. If the signal level on a photodiode suddenly changes then it can take a while (several frames) for the equilibrium to be re-established. If the light level suddenly decreases then we have 'discharging lag', seen as 'comet tails' on bright parts of the image or as residual 'ghost' images. If the light level suddenly increases then we have 'charging lag' where parts of the image are darker than they should be (resulting in 'dead zones'). A by-product of soft reset is that the readout noise is often reduced (kTC noise is usually reduced by a factor √2).

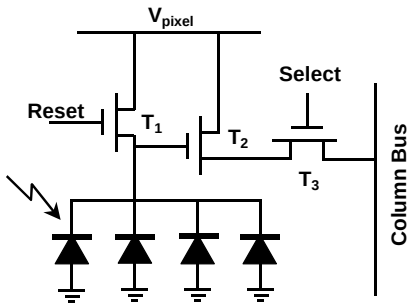

Fig.1 Block diagram of a STAR-250 pixel, showing the four photodiodes and the three transistor readout structure.

The datasheet suggests, as a default, to have both V_{pixel} = V_{reset} = 5.0 V. This implies that the reset transistor will be in weak inversion for small signals. A modification was made to the test electronics to allow V_{pixel} to be varied. It was found that the lag effect was eliminated for V_{pixel} values below 3.8 V. This was checked by using an LED flash synchronized to the APS timing, and capturing multiple images.

However there are four principle drawbacks in using a reduced V_{pixel} voltage: 1) there is a reduction in saturation level (both in terms of signal charge and output voltage), 2) reduction in gain, 3) departures from linearity and 4) changes in the fixed pattern offsets. All of these are more pronounced as V_{pixel} values approach 2.5 V. Figs 2 to 4 illustrate these effects. It is possible that readout noise may also be affected but this has not been measured in detail and only an upper limit can be given (< ~ 50% change in readout noise).

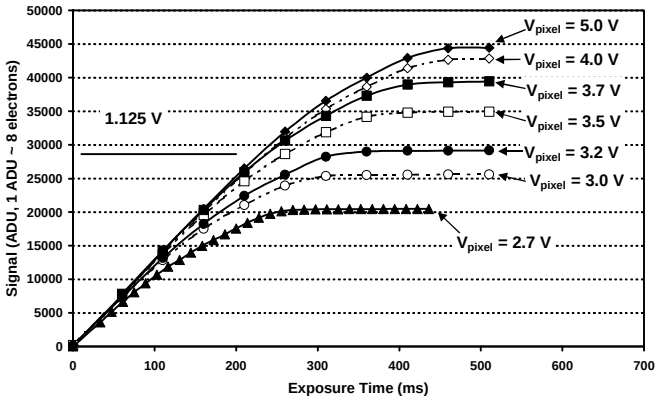

Fig. 2 Changes in linearity and full well voltage with V_{pixel}. The onset of saturation (i.e. the full well charge – since the illuminance was kept constant) also decreases as V_{pixel} is reduced.

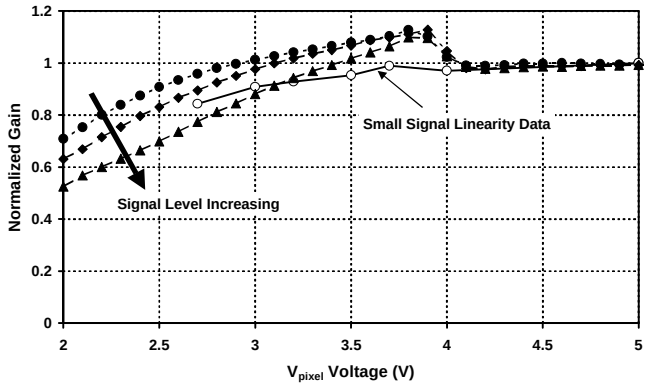

Fig. 3 Change in gain with V_{pixel} , 1) filled symbols: measured by keeping the exposure constant and monitoring the signal as a function of V_{pixel}. and 2) open circles: measured at small signals by finding the initial slope of the linearity plots in Fig. 2.

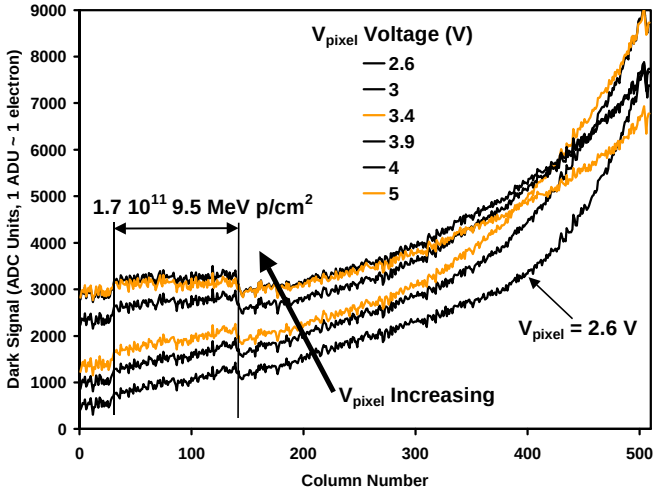

Fig. 4 Variation of dark signal across the array (average of all pixels in each column of the sensor array). Apart from the proton irradiated region, the dark signal is due to fixed pattern offsets (the thermal dark current from unirradiated regions is negligible). The range of fixed pattern offset variation tends to decrease as V_{pixel} is increased.

At the lower values of V_{pixel}, there is a significant reduction in the size of proton-induced dark current spikes. This is shown in Fig. 5, which depicts the variation of individual pixels (the brightest pixels in the irradiated region). It is seen that the dark current spikes almost completely disappear for V_{pixel} values ~ 2.7 V or less. Hence there is a significant radiation hardening effect.

B. Proton-induced Dark Signal

Figs 6 and 7 show the variation in bulk dark current for both the 1.7 10^{11} and 1.7 10^{10} p/cm^2 regions. The counts for V_{pixel} = 5 V have been reduced by a factor 10 for clarity (so that the histograms are displaced vertically). The dark current is extremely nonuniform and there are several 'hot' pixels, the largest being of order 5 10^5 electrons/pixel/s at 17°C (Fig. 7). However the number of high dark current pixels is small (even after the 1.7 10^{11} proton irradiation), presumably because of the small size of the photodiodes within a pixel (large dark currents are only produced in high field regions within the photodiode [7]). The histograms were obtained by subtracting the fixed pattern noise offsets (which are independent of integration time). This was done by taking images with a 55 ms integration time (the time taken for a normal readout of a whole image at 5 MHz pixel rate) and subtracting images obtained with a short (electronically shuttered) integration time of ~ 1ms (the photodiodes were reset 1 ms before readout so as to reduce the integration time). It was found that at high V_{pixel} voltages the short integration mode was not fully functional and the resulting dark currents were underestimated. This is the reason why the V_{pixel} = 5 V histograms are slightly to the left (lower dark currents) of the 2.7 V histograms.

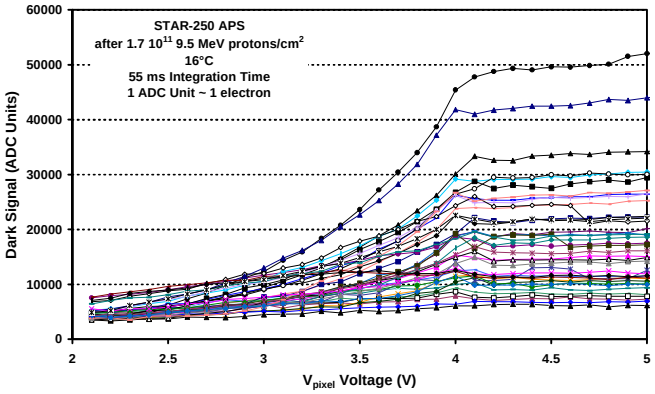

Fig. 5 Variation of proton-induced dark current 'spikes' with V_{pixel}. For low values the dark current spikes are essentially eliminated.

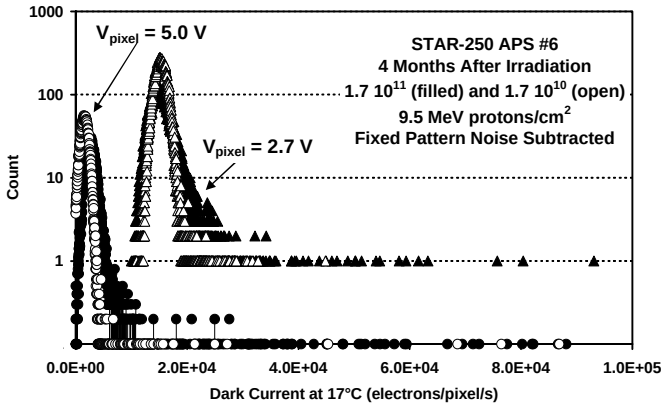

Fig. 6 Dark current histograms for a proton irradiated device at two values of V_{pixel}. The counts for V_{pixel} = 5.0 V have been divided by 10 for clarity.

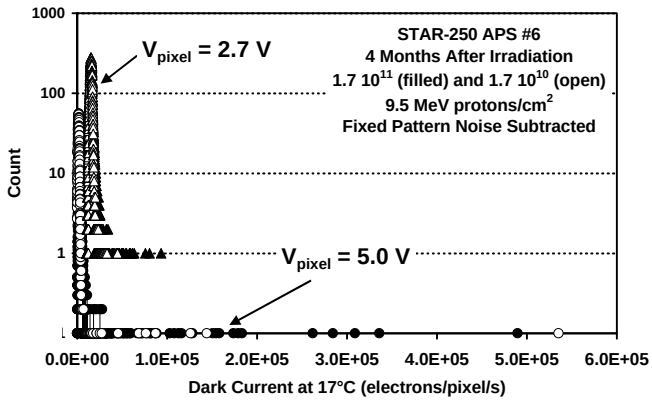

Fig. 7 As Fig.. 5, but showing the full range of dark current

One proton-irradiated device was given a bake at 84°C for 3 days but there was very little change in the dark current. A higher temperature (in the range 110-150°C) is expected to be needed before significant annealing of bulk dark current defects is seen [16].

Measurements were also made of random telegraph signal (RTS) behaviour in the photodiode dark currents. Results were similar to those reported in Bogaerts et al. [8] at 5V V_{pixel} voltage, but if this was reduced to 2.7 V then nearly all the dark current spikes, and hence RTS effects disappeared. At 2.7 V, random samples of 250 pixels in the 1.7 10^{11} p/cm^2 region showed only about 15 low amplitude RTS pixels and in the 1.7 10^{10} p/cm^2 region only the occasional 1 or 2 RTS pixels. If the highest amplitude spikes were selected for the whole of the 1.7 10^{11} p/cm^2 region then roughly half showed RTS behaviour (Fig. 8). Though, as mentioned above, the number of these large spikes is small.

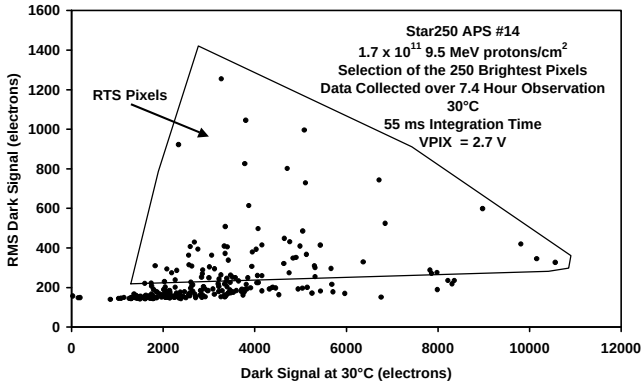

Fig. 8 RTS pixels can be identified by high RMS values, V_{pixel} = 2.7 V.

C. *Cobalt60-induced Dark Current*

Cobalt60 gamma rays will induce very little displacement damage but will cause an increase in surface dark current. A dark current image from a cobalt60 irradiated device is shown in Fig. 9 and data is plotted as a function of inverse temperature in Fig. 10. It is seen that the dark current is nonuniform and is higher at the centre of the chip than in the corners. The reason for the nonuniformity is unknown but it presumably arises as a result of device manufacture. The dark signal is thermal in character and shows an activation energy of 0.65 eV. In contrast, many of the larger proton-induced dark current spikes show a reduced activation energy characteristic of field enhancement (this is discussed in detail in [7]). Immediately after irradiation the dark current was higher for devices irradiated under bias, but after annealing (8 months storage at room temperature and 3 days at 84°C, both unbiased) the dark current from the unbiased device increased to a similar level as the biased ones. The peak dark current increase (centre of image) amounts to ~ 3.7 pA/cm^2/krd(Si) at 20°C (25 µm x 25 µm pixel). This is similar to the average value of 1.5 pA/cm^2/krd(Si) at 20°C found in [3] after 5.3 Mrd(Si), bearing in mind that the average is about 50% of the peak value. In [4] Bogaerts et al. found a comparable increase but saw a logarithmic behaviour (above a threshold dose). A possible explanation is that their data is influenced by image lag effects.

The fixed pattern noise (dark signal at low temperatures or short integration time, due to electronic offsets) was not seen to change significantly with irradiation, in agreement with [4]. The fixed pattern offsets were found to be slightly temperature sensitive.

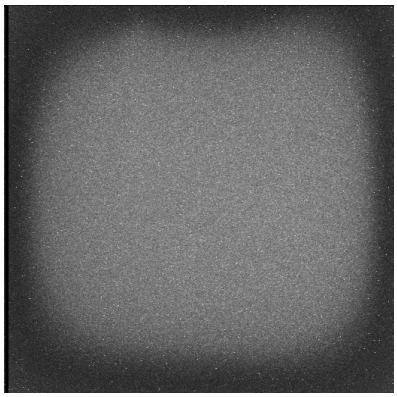

Fig. 9 Dark image from a cobalt60 irradiated device

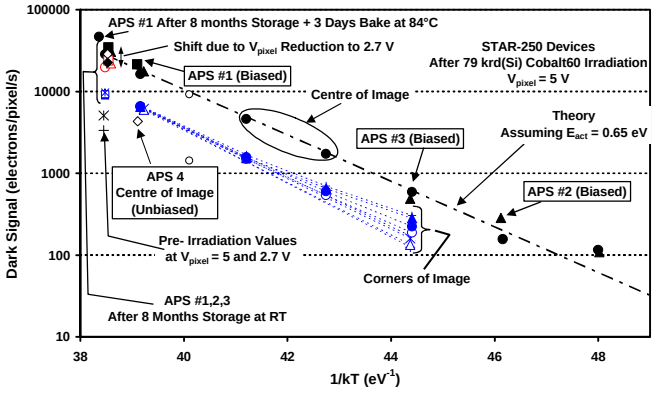

Fig. 10 Dark signals from cobalt60 irradiated devices

D. *Changes in responsivity*

Changes in responsivity were observed after both cobalt60 and proton irradiation (as also reported in [4]). Fig. 11 shows a flat field image (white light illumination) for a proton irradiated device. The reduction in response for the 1.7 10^{11} p/cm^2, 100 krd(Si), region (left hand dark area) and the 1.7 10^{10} p/cm^2, 10 krd(Si), region (right hand dark area) can be seen clearly. Fig. 12 displays the relative responsivity values, which did not significantly change after annealing. After 80 krd(Si) cobalt-60 the reduction in responsivity was roughly a factor 2 for all devices (independent of irradiation bias) and in agreement with the proton data. However, there appears to be a saturation effect in that the responsivity decrease after 5.3 Mrd(Si) cobalt-60 [3] remained at the level of a factor 2. The shape of the spectral response did not change after irradiation – only the absolute responsivity (Fig. 13); hence the changes were not sensitive to the wavelength of the illumination and are believed to be mainly due to a reduction in the gain of a pixel. This was confirmed by Cd109 X-ray measurements which showed a reduced signal size for the irradiated regions of the proton irradiated devices (Fig. 14) – though the change was not as large as the reduction in

responsivity, suggesting that there may also be a (wavelength independent) change in the photodiode collection efficiency. In [3] the responsivity was also measured for narrowband green and red filters but the results were inconclusive. It can be seen from Fig. 13 that the spectral response shows deep modulations due to the surface structure. These modulations vary between devices and this explains the anomalous results with colour filters found in [3].

Fig. 11 Flat field image from a proton irradiated device, the irradiated regions can clearly be seen as dark areas.

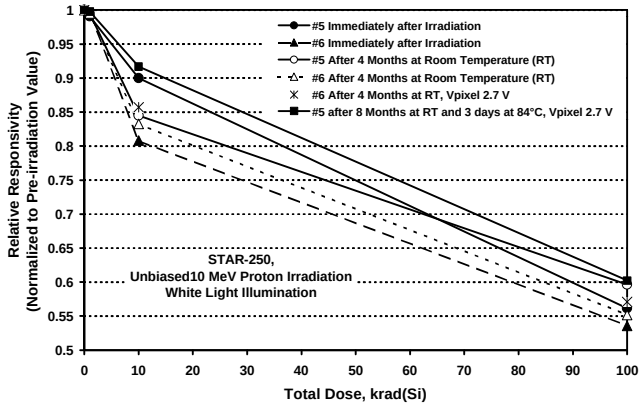

Fig. 12 Relative responsivity versus 9.5 MeV proton total ionizing dose

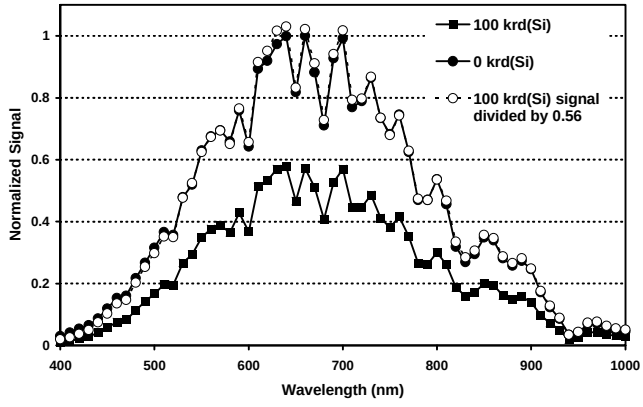

Fig. 13 Spectral response, before and after proton irradiation

Fig. 15 shows an image obtained with a proton irradiated device. A rectangular 'area of interest' was placed around the

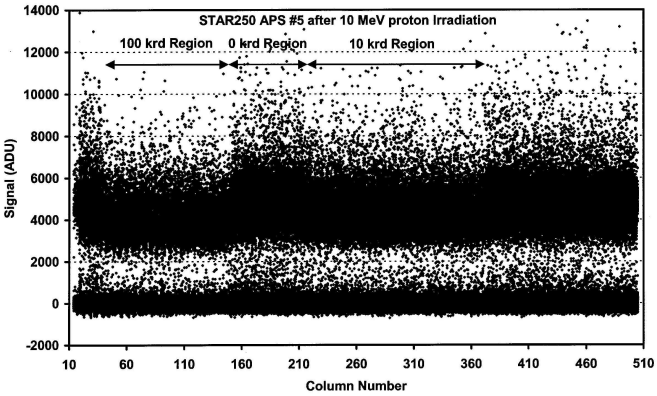

Fig. 14 Plot of signal from Cd109 X-ray events (stacked line trace). The signal in the irradiated regions is noticeable reduced, suggesting a change in transistor gain within the pixel.

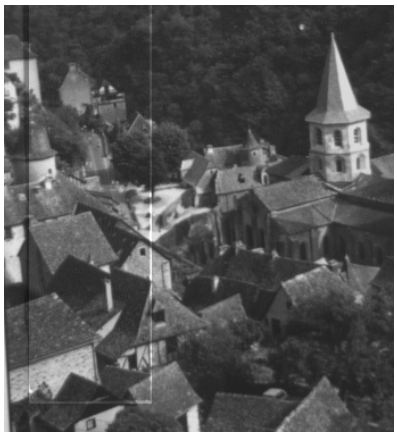

Fig. 15 Image from a proton irradiated device. The signal in the rectangular area on the left (100 krd) was divided by 0.62 to compensate for the change in responsivity.

100 krd(Si) region and the signals in this area divided by a factor 0.62. It can be seen that this gives good compensation for the responsivity change. It should be emphasized that, although the effects were easiest to demonstrate with the proton irradiated devices, we believe the effect to be due to total ionizing dose (as a similar change is also seen with cobalt60 gammas, as mentioned above).

E. Photo-response Nonuniformity (PRNU)

The photo-response nonuniformity (PRNU) tends to be dominated by low spatial frequency fringes or 'swirl patterns'. The amplitude of these is typically 2%. It was found that these patterns did not change appreciably in an absolute (signal voltage) sense after irradiation, but after correction for the responsivity change (~ factor 2 after 100 krd) there is an increase in PRNU. Fig. 16 shows white light flat field images before and after 80 krad(Si) cobalt60 irradiation. The images have been processed to have the same gain but different offsets (the pre-irradiation image has approximately twice the signal). It can be seen that the 'swirl' patterns are very similar. Notice that the responsivity is higher in the corners of the APS after irradiation. This is a similar effect to the reduced damage in the corners seen in the dark image of Fig. 9.

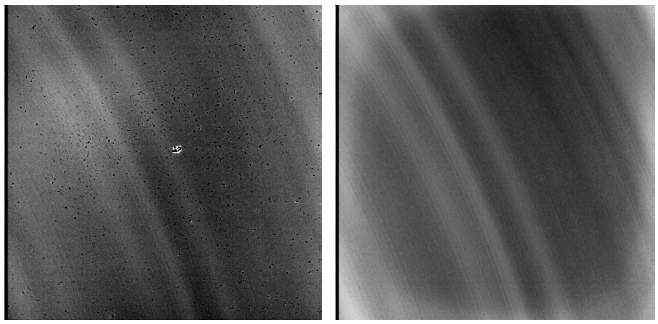

Fig. 16 Flat field images before (left) and after (right) 80 krd(Si) cobalt60 irradiation. The amplitude of the 'swirl' patterns is unchanged even though the average responsivity has decreased by a factor ~ 2.

F. Threshold Voltage Shift

The clock voltages applied to the devices were varied under computer control in 50 mV steps and the values at the transition between device operating and non-operating states were recorded. There was negligible change after 80 krad(Si) cobalt60, in line with the results in [3] were a shift of only 80±20 mV was found after 5.3 Mrd(Si). This result is expected since total dose effects in the thin (10 nm) gate oxide should be small. This means that the APS voltages do not need adjustment during or after irradiation.

G. Power Supply Currents

Measurements of both the sensor and on-chip ADC currents were made during the 80 krd(Si) cobalt60 irradiations and for several months afterwards. The sensor currents increased slightly from ~ 22 mA to 29 mA but annealed back to the starting value after 8 months unbiased at room temperature. The change in ADC current was small and within the ~ 2 mA measurement error (the starting value was ~ 93 mA at 5 MHz pixel frequency, but is frequency dependant).

H. ADC Performance

Differential and integral nonuniformity (DNL and INL respectively) were measured by linearly increasing the black level reference voltage to the output amplifier (which linearly increases the input voltage to the ADC) while keeping the sensor in the dark. Very little change in ADC performance was seen after 80 krd(Si). Fig. 17 shows typical ADC DNL before (open circles) and after irradiation (filled circles). None of the measurements showed missing codes.

I. Heavy Ion testing

The STAR-250 sensor and ADC currents were continuously monitored during the heavy ion tests and an event could be logged every time the current exceeded a (user selectable) threshold value, at which point the power was automatically cycled and the test resumed. The analogue output was fed to a TV monitor and video recorder so that a record could be kept of any single event interrupts. In fact none were observed up to the maximum LET of 68 MeV/(mg/cm^2) (Kr ions at 60º incidence at a fluence on each device of 1 x 10^6 ions/cm^2) and the images were all of the appearance of Fig. 18, that is, a dark background with 'white spots' due to the transient signals produced by the ionization of the heavy ions. In fact these transients were a useful real time indicator of the ion flux.

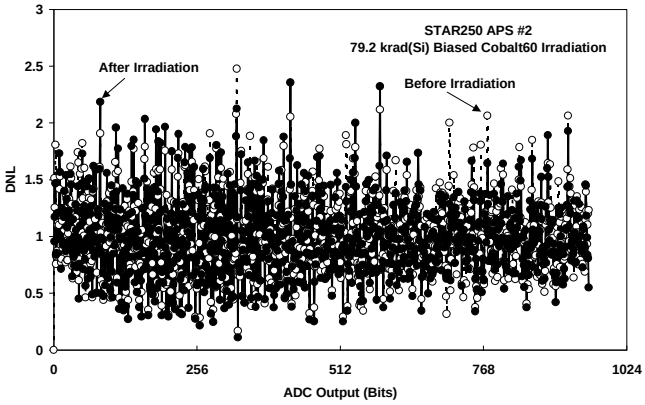

Fig. 17. Differential nonlinearity for the on-chip ADC

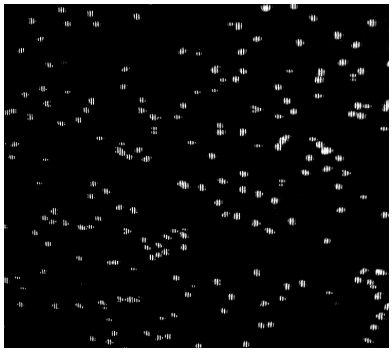

Fig. 18 Transient events observed during heavy ion testing (recorded from a TV monitor fed from a VCR recorder).

The on-chip ADC was not connected to the analogue output of the sensor array, but instead to a DC voltage provided by a DAC. The digitized values were collected by an FPGA on the test board and transmitted to the data logging computer. A log was kept of the histogram of ADC values. If a data value exceeded a user defined level for more than 10 samples then an error would be flagged and the power recycled. This procedure was designed to check for (and correct) any lingering errors (a form of single event functional interrupt). Again, no such single events were observed.

No single event latch up (SEL) was observed in either of the two STAR-250 devices tested, up to the same maximum LET of 68 MeV/(mg/cm^2). In fact here was no increase in current to a measurement accuracy of 0.1 mA. However an increase in noise due to small signal transient events was seen in the ADC data. The noise spreads over roughly ± 40 ADU (out of a full range of 1024 bits). A check was made on an unirradiated device that the noise was not due to the experimental set up at the accelerator.

Two IRIS-2 devices were also tested for SEL. These are active pixel sensors, designed in a similar way to the predecessor of the STAR-250 (the ASCoSS APS), but have an on-chip clock sequencer and data interface so as to form a 'camera-on-a-chip'. Because this device was not specifically

hardened, it was expected to show SEL as in the ASCoSS device [1] and this was, in fact, the case. No latch up was seen at 5.85 MeV/(mg/cm^2) (Ne, 0º incidence) but at 8.27 MeV/(mg/cm^2) (Ne, 45º incidence) and above, SEL was observed. The number of SEL events increasing with particle LET. It was seen that several of the SEL events gave only a small increase in power supply current – small enough to be non-destructive even if the current were not limited. It is not known, however, if the device was still functional during these 'mini-latch' events. Most events had a current of 220 mA or greater (the current limiting circuit reduced the voltage to ~ 3.7 V for this current) but latches of ~ 100 mA were also observed. The typical operating current was 43 mA. A new version of the device (the IRIS-3) has now been developed by the manufacturer, but so far has not been tested.

IV. Discussion

The present study has confirmed the usefulness of the STAR-250 for high radiation space environments and demonstrated the effectiveness of the hardening-by-design approach. The only major change after irradiation was a reduction in responsivity (and associated increase in PRNU) which, unlike the previous device [1] did not anneal after irradiation (even after 8 months storage at room temperature or after a bake at 83ºC for 3 days). However the change after 10 krd(Si) was no more than 10-20% and could be allowed for in the system design. There is a saturation effect at higher doses: a previous study [3] showed that the responsivity change at 5.3 Mrd(Si) was little more than the 100 krd(Si) value found here, which was ~50%. Note that the effect has a similar magnitude for both cobalt60 and proton irradiations and so is likely to be an ionization rather than a displacement damage effect.

It was found that the V_{pixel} supply voltage to the drain of the reset and source follower transistors must be reduced below 4 V for the image to be free from lag effects - though in high signal applications the lag can have a benefit in that small signal transient events are reduced.

Reducing V_{pixel} further gives a large reduction in proton-induced dark current spikes (which at 5 V are large, presumably because of high electric fields present within a pixel). Note, though, that the small area of the photodiodes (they are much smaller than the area of a pixel) means that the number of spikes, and the average dark current value, is low. The reduction in dark current spikes gives an important radiation hardening effect. However, the trade-offs with gain, linearity, full well capacity and noise will need to be studied in detail for each application.

The heavy ion test showed that the device was immune to latch-up up to the maximum test LET of 68 MeV/(mg/cm^2). No single event upsets or functional interrupts were seen in the array shift registers or the on-chip ADC, though there was an increase in ADC noise transients.

The IRIS-2 device showed latch-up events at 8.27 MeV/(mg/cm^2), but not at 5.85 MeV/(mg/cm^2), with a variety of currents, suggesting a 'mini-latch' effect. The testing was not configured to establish if imaging capability could be maintained during these events, which were non-destructive. It is suggested to include such tests during future heavy ion irradiation of similar devices. A challenge for the testing of complex imaging devices, such as active pixel sensors, is to include measurements for all the possible effects of radiation. The present study illustrates the types of effects that can occur and, with the inclusion of imaging tests during heavy ion irradiation, should provide an adequate test methodology for future devices.

V. Acknowledgment

The help of Guy Berger (LLN), Keith Jones (Ebis Iotron Ltd) and Bob Nickson (ESA) in performing the irradiations is gratefully acknowledged.

VI. References

[1] G. R. Hopkinson 'Radiation effects in a CMOS active pixel sensor', IEEE Trans. Nucl. Sci., vol. 47, pp. 2480-2484, Dec 2000.

[2] J. Bogaerts and B. Dierickx, 'Total dose effects on CMOS active pixel sensors', Proc SPIE, vol.3965, pp 157-167, January 2000.

[3] G. R. Hopkinson, M. D Skipper and B. Taylor 'A radiation tolerant video camera for high total dose environments', Workshop Record, 2002 IEEE Radiation Effects Data Workshop, IEEE 02TH8631, pp 18-23, 2002.

[4] J. Bogaerts, B. Dierickx, G. Meynants and D. Uwaerts, 'Total dose and displacement damage effects in a radiation hardened CMOS APS', IEEE Trans. Elec. Dev., vol. 50, no. 1, pp. 84-90, Jan 2003.

[5] G. R. Hopkinson, D. J. Purll, A. F. Abbey, A. Short, D. J. Watson and A Wells, 'Active pixel array devices in space missions', Nucl. Phys. and Meth. In Phys. Res., vol. pp. 2003.

[6] E.-S. Eid, T. Y. Chan, E. R. Fossum, R. H. Tsai, R. Spagnuoto, J. Deily, W. B. Byers Jr., and J. C. Peden, 'Design and characterization of ionizing radiation-tolerant CMOS APS image sensors up to 30 Mrd(Si) total dose', IEEE Trans. Nucl. Sci., 48, no. 6, pp 1796-1806, Dec 2001.

[7] J. Bogaerts, B. Dierickx and R. Mertens, 'Enhanced dark current generation in proton-irradiated CMOS active pixel sensors', IEEE Trans. Nucl. Sci., vol. 49, no. 3, pp 1513-1521, Jun. 2000.

[8] J. Bogaerts. B. Dierickx, and R. Mertens, 'Random telegraph signals in a radiation-hardened CMOS active pixel sensor', IEEE Trans. Nucl. Sci., vol. 49, no. 1, pp 249-257, Feb. 2002.

[9] M Cohen and J.P. David, 'Radiation-induced dark current in CMOS active pixel sensors', IEEE Trans. Nucl. Sci., Vol. 47, pp. 2485-2491, Dec. 2000.

[10] C.J. Marshall et al. 'Heavy Ion Transient Characterization of a Hardened-by-Design Active Pixel Sensor Array', Workshop Record, 2002 IEEE Radiation Effects Data Workshop, IEEE 02TH8631, pp. 187-193, 2002.

[11] X. Belredon, J.-P. Davis, D. Lewis, T. Beauchene, V. Pouget, S. Barde, and P. Magnan, 'Heavy Ion-Induced Charge Collection Mechanisms in CMOS Active Pixel Sensor', IEEE Trans. Nucl. Sci., Vol. 49, pp. 2836-2843, Dec. 2002.

[12] B. R. Hancock, T. J. Cunningham, K. McCarty, G. Yang, C. Wrigley, P. G. Ringold, R. C. Stirbl and B. Pain, 'Multi-megarad (Si) radiation tolerant integrated CMOS imager', Proc SPIE, vol. 4306, pp. 147-155, 2001.

[13] Datasheet from http://www.fillfactory.com/htm/cmos/htm/star.htm

[14] H. Tian, B. Fowler and A. El Gamal, 'Analysis of temporal noise in CMOS photodiode active pixel sensor', IEEE J. Solid State Cir., vol. 36, no. 1, pp. 92-101, 2001.

[15] E. R. Fossum, 'Charge transfer noise and lag in CMOS active pixel sensors', 2003 IEEE Workshop on Charge-Coupled Devices and Advanced Image Sensors, Elmau, Germany, 2003.

[16] G. R. Hopkinson and A. Mohammadzadeh, 'Comparison of CCD damage due to 10 and 60 MeV protons', presented at the IEEE 2003 Nuclear and Space Radiation Effects Conference, Monterey, CA, July 2003.